The EU Framework Programme for Research and Innovation H2020
Research and Innovation Action

CENTAURO

Deliverable D2.5 Final version of Centauro Robot

Dissemination Level: Public

Project acronym:	CENTAURO
Project full title:	Robust Mobility and Dexterous Manipulation in Disaster Response by Fullbody Telepresence in a Centaur-like Robot
Grant agreement no.:	644839
Lead beneficiary:	IIT – Fondazione Istituto Italiano di Tecnologia
Authors:	Navvab Kashiri, Lorenzo Baccelliere, Luca Muratore Nikos Tsagarakis
Work package:	WP2 – Robot Platform
Date of preparation:	2018-9-18
Type:	Report, Prototype
Version number:	1.0

Document History

Version	Date	Author	Description
0.1	2017-09-21	Navvab Kashiri	Initial version
1.0	2018-10-8	Navvab Kashiri	first revised version

Executive Summary

Deliverable D2.5 presents the final version of the CENTAURO robot based on the previous deliverables on this work-package, and also the robot updates including a number of actuation gearing changes, cooling unit revisions, electronics upgrades and pelvis units re-arrangements. This deliverable describes the robot design briefly, including the kinematics of head, arms and legs. It also reports the actuation units of the robot, and lists the computational, communication and power autonomy units of the robot. The control architecture of the robot is also shortly reported.

Contents

Figure 1: Final version of the CENTAURO robot.

1 Introduction

The workpackage WP2 focuses on the development and experimentation of the CENTAURO robot platform. To this end, the main target of the workpackage is to design and fabricate all mechanical and electrical components, and eventually assemble them to realize the first CENTAURO robot prototype in two design iterations. In particular within WP2, the main goal of the Task T2.1 is the design and realization of the CENTAURO robot, while that of the Task T2.2 is the construction and assembly of the robot platform. Based on the project objectives and desired functionalities, including locomotion and manipulation in unstructured workspaces, payload capacity, and interaction with the environment, the robot specifications were derived and the design requirements were defined. To achieve this, the design activity started during the first period of the project, and following to the development of CENTAURO upper body, the robot lower-body was devised. This comprises the development of compliant actuation system powering the robot joints, including both arm and leg actuators, as well as the design and realization of a torso module, two manipulator arms, four wheeled legs, and a head encompassing the major part of the robot perception unit.

As an outcome of the aforementioned tasks T2.1 and T2.2, the first prototype of the CENTAURO robot was released in D 2.3 [1]. This reports describes the robot design including the updates with respect to the first prototype, including a number of actuation gearing changes that allows for higher torques at leg joints, cooling unit revisions enabling long time operations, electronics upgrades guaranteeing reliable communications, and pelvis units re-arrangements preventing interference of legs and battery; towards the final version of the CENTAURO robot shown in Fig. 1. The document presents description and details on the solution employed for enhancement of the platform integration and performance.

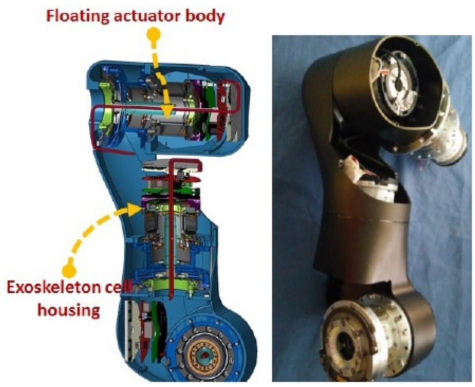

Figure 2: The exoskeleton cell structures and floating body principle.

Figure 3: Leg sections with revised cells/fans.

2 Centauro Robot Body

The robot design followed an exoskeleton structure approach to connect the actuators to body structures. Exoskeleton cells have higher structural stiffness and minimize the effect of unmeasured elasticities. Fig. 2 illustrates the principle of the structure and actuation integration, in which the body of the actuators are floating inside this exoskeleton structure while the actuator is fixed to the link structures. As it can be seen, the actuation modules are mechanically interfaced to the exoskeleton cell links using two standard flange interfaces, one fixed to the previous link and the other to the subsequent link. The exoskeleton structure and floating actuation integration approach offers several advantages with respect to the more traditional exoskeleton interconnection between the actuators and the robot links. Actuator bodies are not subject to loading as torques and forces generated from the joint loading or due to interactions, are transmitted only through the two output flanges used to fix the actuator to the structure cell. It therefore allows for optimal and low-weight design of the actuation housing components that are not subject to the joint loading. It is an explicit design feature that the link cells form a wind tunnel around the actuation body that can be used for forced air cooling.

To allow for long operations of the robot while executing demanding tasks, the leg's cooling system were upgraded with larger fans and revised cells providing the drive units with an increased air flow and faster heat dissipation, and accordingly longer peak operations. Fig. 3 presents two of joints with larger fans and revised associated ABS cells. Following to this upgrade, a set of experiment involving 15 minutes of continuous squat motions were carried out and the results were presented in D 8.3 [2]. The results demonstrated this upgrade enables the robot to perform such a torque demanding task without any considerable temperature increase in motors.

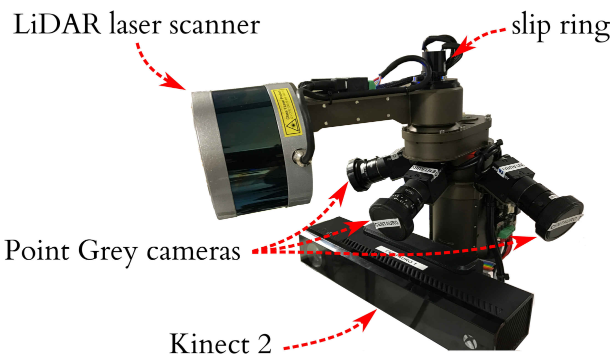

Figure 4: Head module.

2.1 Vision-Perception Systems

The main vision-perception subsystem of the CENTAURO robot is the head module that is placed on top of the torso unit, and encompasses a set of cameras and sensors, as illustrated in Fig. 4. It includes: 1. A two-DOF mobility platform for a Kinect 2 sensor, at the bottom layer, to generate yaw and pitch motions of this RGB-D sensor, respectively; 2. A structure for an array of three colour cameras (PointGrey BlackFly BFLY-U3-23S6C wide angle cameras), at the middle layer, to install these cameras to the head base; and 3. A continuous rotation single DOF support beam for a 3D LiDAR sensor (Velodyne PUCK sensor), at the top layer, to provide spherical coverage of the environment around the robot. Moreover, two additional RGB cameras are mounted under the robot base to get a view on the feet.

Moreover, a pair of customized force-torque sensors between the arm wrists and the hands measures 6D forces/torques which are applied to the end-effector and can be used for force feedback by the exoskeleton. To enhance the reading and communication quality of Force/Torque (FT) sensors, the electronics module of these units are upgraded with a more efficient power supply, rendering measurements with lower noise and higher communication reliability.

3 Robot Legs

To allow for versatile locomotion, each leg consists of five DoF in a spider-like configuration, which can be more beneficial in terms of stability required for the manipulation of powerful tools, as shown in [12]. Furthermore, in this configuration, the first leg joint has to deliver substantially lower effort and power compared to a mammal-like configuration. According to the chosen spider-like configuration, each hip module consists of a yaw and a pitch joint, followed by another pitch joint in the knee. Each ankle consists of a pitch and a yaw joint which allow for steering the wheel and adjusting its steering axis to the ground. Finally, each leg ends in an actively drivable wheel. The described configuration allows for omnidirectional driving as well as for articulated stepping locomotion. Since no posture change is needed to switch between the two, it is even possible to perform motions which are unique for that design such as moving a foot relative to the base while under load. Thus, a wide range of locomotion capabilities is provided. To permit versatile leg articulation in difficult terrains, the ranges of the leg joints were maximized while taking into account the mechanical and electrical interfacing constraints.

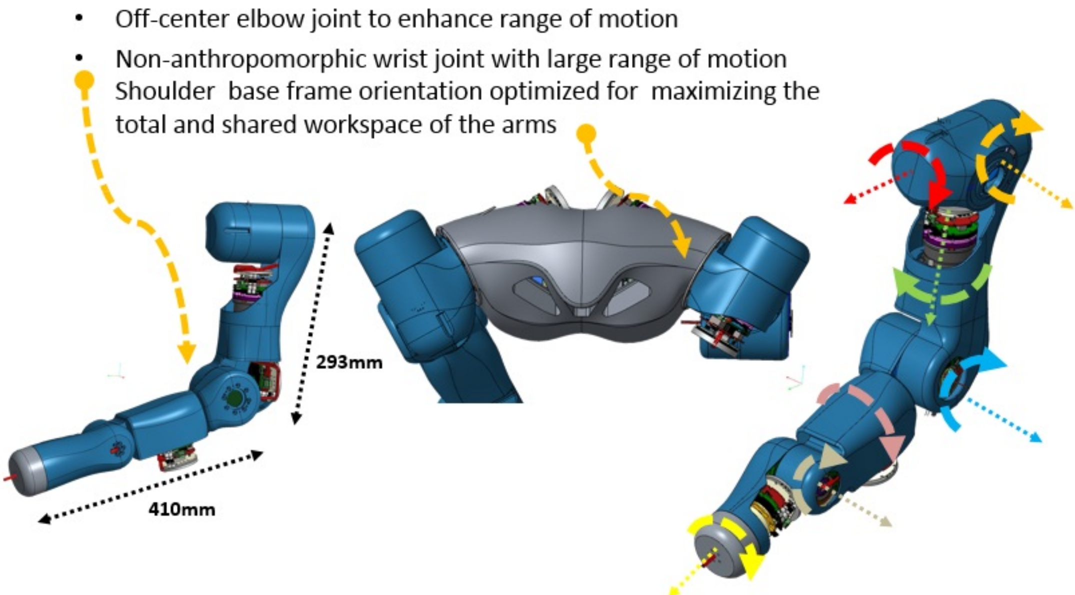

Figure 5: Arm kinematic features.

4 Robot Arms

The robot torso incorporates two arms with seven DoF each and an additional rotational joint in the waist, to endow the upper-body with yaw rotation, as shown in Fig. 5. The kinematics of the two arms closely resembles an anthropomorphic arrangement to provide a large workspace, to enable dexterous manipulation, and to simplify teleoperation. Each arm is 73 cm long and comprises of three DoFs at the shoulder, one DoF at the elbow and another three DoFs at the wrist. The degree of redundancy helps to overcome possible constraints that may be introduced in the task space by the surrounding environment. Even though this is a traditional design that aims at replicating the anthropomorphic structure of the human arm with seven DoF, it is only approximately equivalent for the human arm kinematic structure. To extend the range of motion of the elbow joint, an off-center elbow configuration was chosen. Similarly, for the wrist, a non-anthropomorphic configuration with non-intersecting axes was considered to maximize the range of motion of the wrist flexion and abduction motions. Finally, humans have the ability to elevate (upward/downward) and to incline (forward/backward) the shoulder joint, utilizing supplementary kinematic redundancy of the arm to achieve certain goals in task coordinates. This, however, would require the addition of two more DoF to each arm, increasing the complexity/weight and dimensions of the overall platform. To avoid this, while at the same time obtain, to some extent, the benefits provided by the elevation (upward/downward) and inclination (forward/backward) of the shoulder, a fixed elevated and inclined shoulder arrangement was selected based on the optimization study in which important manipulation indices were considered and evaluated in a prioritized order [7].

5 Centauro Robot Actuation

Having defined the kinematics of the limbs, the required actuation performance for each joint could be derived. To get an estimation of the actuation needs satisfying the requirements defined in KHG meeting [9], a series of simulation studies was executed using an initial model of the robot based on estimated rigid body dynamic properties [10]. A set of trajectories with different

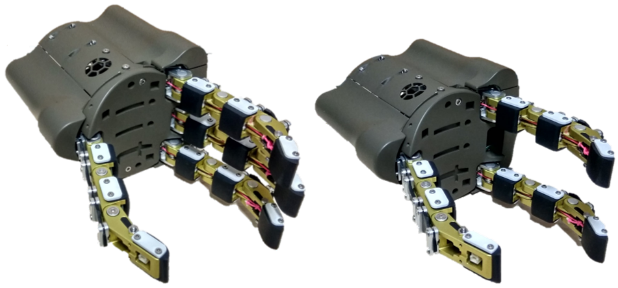

Figure 6: HERI II Hand in two configurations

frequencies which explored the overall robot workspace was executed, while carrying a 10 kg payload per arm. Respective joint torques were examined, resulting in the identification of a set of actuator classes with different sizes and torque levels ranging from about 30 to 270 Nm.

The series-elastic actuation (SEA) technology is utilized to protect the reduction gear against impacts-improving the system sturdiness, while at the same time being used for measuring the actuator torque through the monitoring of the elastic element deflection. Considering the influence of different joints' stiffness levels on the natural dynamics and control of the robot, as discussed by [11], and taking into account the available space for the different actuators, two technologies were utilized for joint torque measurement based on strain-gauge and deflection-encoder principles [8]. The stiffness of the SEA deflection-encoder-based sensor is defined with respect to the required torque measurement resolution across the different joints. It was set ten times lower than the cogging torque of the motor drive when deflection of the sensor flexure is measured using a high resolution 19-bit absolute encoder.

6 CENTAURO Manipulation End-effectors

The two arms end in different end-effectors with complementary properties to provide an overall wide range of manipulation capabilities. On the left arm, HERI II hand with four DoFs provides compliant and robust manipulation, while the right arm utilizes an anthropomorphic Schunk hand with nine DoF for dexterous manipulation tasks. Below, the HERI II hand developed within this work-package, as well as its integration into the CENTAURO arm, is described.

Different types of under-actuated hands have made great progress in terms of anthropomorphic hardware design in low cost and robust grasping. However, due to the simplification in finger design and reduction in degrees of actuation, the majority of under-actuated hands are incapable of executing even basic dexterous motions such as pinching, triggering and thumb abduction/adduction. Furthermore in most under-actuated hands, the mechanical transmission system couples one actuator to several fingers, such a coupling adds complexity in the transmission routing, reduces the robustness and mechanical efficiency as well as hinders the regular maintenance. Motivated by the limitations of under-actuated hands, we developed in [3] a novel hand design in such a way that the finger distribution and quantity could be configured based on different application requirements, see Fig. 6.

The dexterous performance of the hand is firstly demonstrated by holding the drill and repeatedly triggering the power on button, which fully utilized the dexterous property in terms of controlling each finger module independently. The hand was also controlled to precisely pinch objects on the table, such as a pen as presented in Fig. 7. Moreover, the mechanical transmission between the under-actuated finger and the actuator is designed to deliver high efficiency and maintenance convenience. Intrinsic elasticity integrated in the transmission system make the

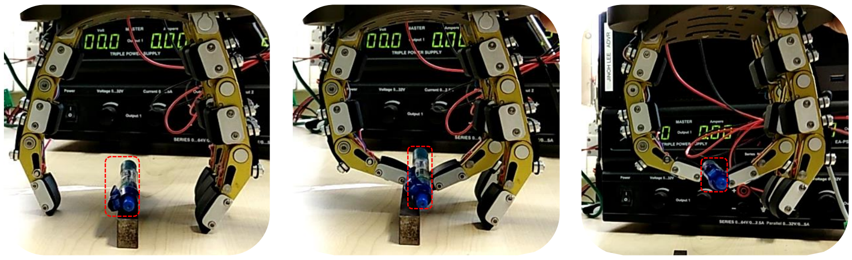

Figure 7: Precisely pinch a pen from table.

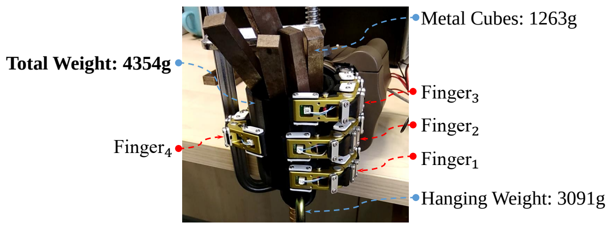

Figure 8: Vertical grasping experiment and finger naming order

hand robust and adaptive to impacts when interacting with the objects and environment.

Fig. 8 shows an experiment of the hand vertically grasping a cylinder object of 75 mm diameter and 4354 g weight. Another experiment was performed by controlling the hand to grasp a hammer and execute the task of knocking a nail in a wood block as depicted in Fig. 9. The disturbance during knocking nail applied on four fingers can be detected from contact force curves in plots, where the specific finger naming order could be refer from Fig. 8, with phalanx_1, phalanx_2 and phalanx_3 being the closest, middle and furthest phalanx w.r.t. the palm, respectively.. The impact effects can be obviously noticed on fingers, demonstrating the robust grasping of the proposed hand and its physical resilience to impacts.

To achieve the configurable finger distribution and quantity, and improve the electronics and mechanics integration of the whole hand, fingers are designed to be independent and identical modules with individual actuation. Since the grasping algorithms and kinematics analysis for the under-actuated finger highly depend on its structure, the utilization of identical finger modules will improve the standardization of hardware and facilitate the general applicability of different grasping algorithms. As an end-effector for the Centauro robot arm [5], we adapt the design with the robot forearm in a way that a compact design embodying essential components is achieved. Fig. 10 reveals the HERI II Hand's integration with the Centauro forearm.

7 CENTAURO untethered operation Units

To allow for better integration of modules in the robot trunk, the core components are arranged as shown in Fig. 11.

7.1 Computation units

As shown in the schematics image of higher-level components interconnection in Fig. 12, the CENTAURO robot includes three computation units initially placed inside the pelvis, one responsible for the Real-Time control of the robot and running with XENOMAI RT

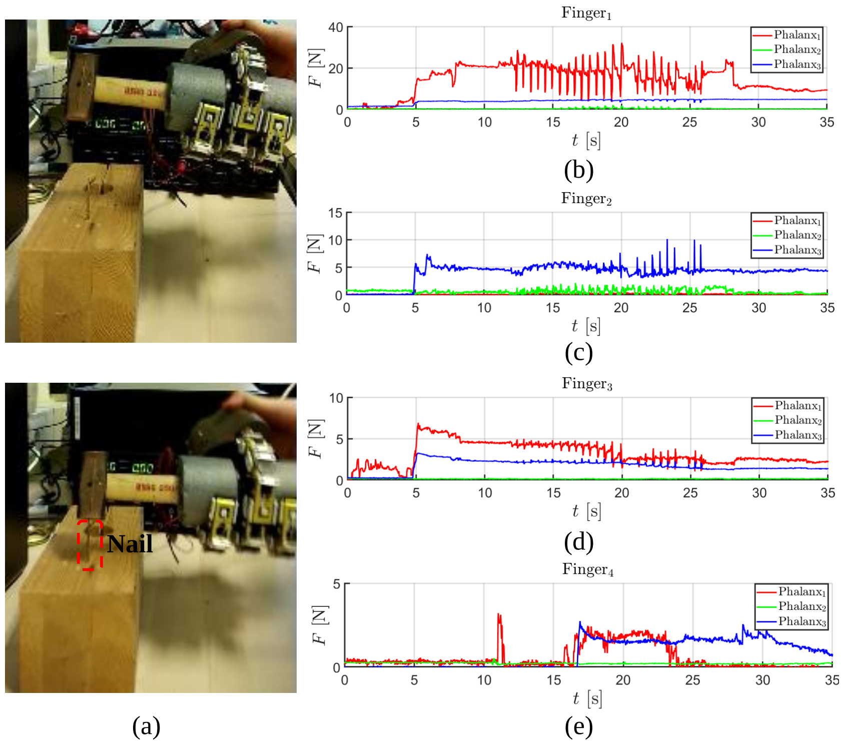

Figure 9: Powerful grasping a hammer during the high impact knocking nail task.

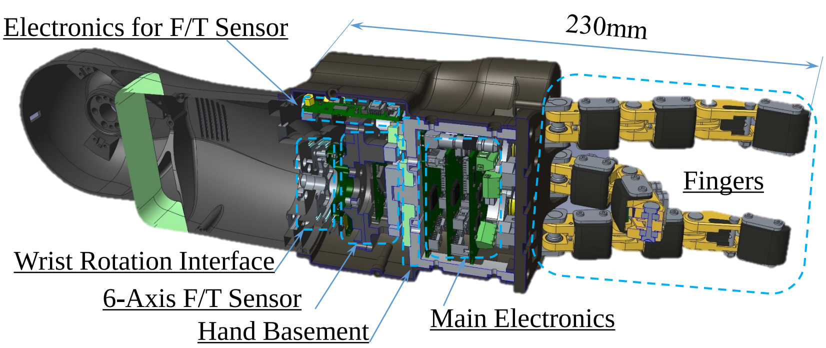

Figure 10: HERI II Hand cross section showing the integrationof the various electronics and F/T sensor.

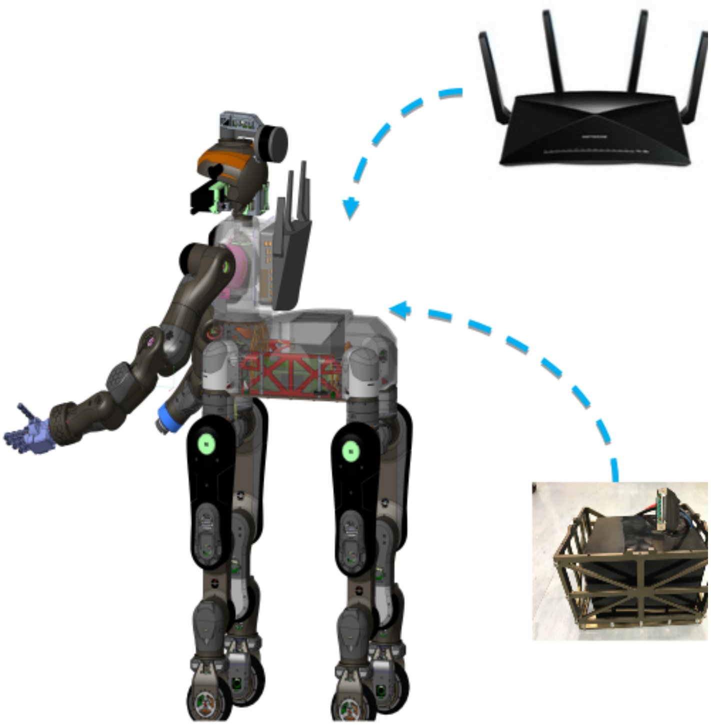

Figure 11: Arrangement of components in the robot trunk.

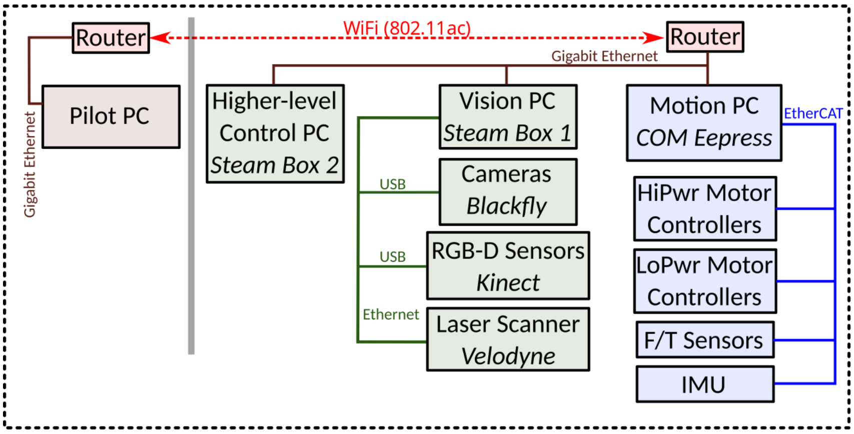

Figure 12: Higher-level schematics of the interconnections of the final CENTAURO robot control and perception components.

development kit[1], and the other two used for perception and high level robot control, with the specification reported in Table 1 and 2. To adapt with the placement of the battery inside the pelvis, one of vision PCs (Steam Box 1) and the motion PC (COM Express) was placed out of the pelvis. The motion PC is located at the front-side center of the torso, as shown in Fig. 13, where a fresh air flow for cooling of this PC is available. The vision PC is on the other hand, is placed at the back-side center of the torso, between the torso and the wireless communication router so that a more convenient connection of vision components and this PC can be attained.

[1] `https://xenomai.org/`

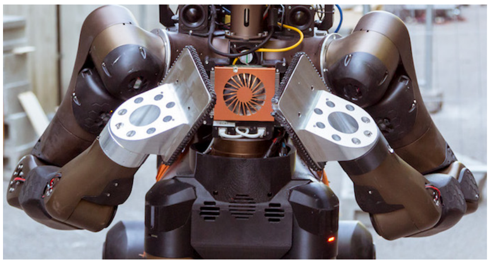

Figure 13: Front-side view of the CENTAURO robot showing the COM Express PC at the torso center (in orange).

Table 1: CENTAURO RT on-board computational unit hardware specifications.

COM Express Type 6	Conga-TS170
CPU	Intel Core i7-6820EQ 2.80GHz up to 3.50GHz 4 cores (2 logical cores per physical) TDP: 45 W
SSD	120GB
RAM	16GB

Table 2: CENTAURO on-board perception and high level robot control unit hardware specifications.

ZOTAC MAGNUS	ZBOX-EN1070K
CPU	Intel Core i5-7500T 2.7 GHz, up to 3.3 GHz 4 cores (2 logical cores per physical) TDP: 35 W
GPU	GeForce® GTX 1070 8GB GDDR5 256-bit
SSD	500GB
RAM	32GB

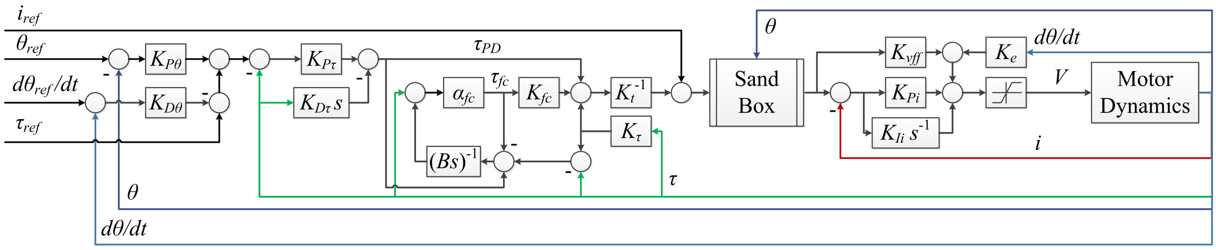

Figure 14: Block diagram scheme of the joint controllers: current feedback in red, torque feedback in green, position and velocity feedbacks in blue.

7.2 Battery

The robot carries a 7.5 kg Lithium-Ion polymer battery of 34.6 Ah capacity supplying 48 V with 80 A max current discharge (limited by PCM), permitting about two hours power autonomy for standard manipulation and locomotion tasks. While the battery was previously caged below the pelvis, the designed is revised to include the battery inside the pelvis cage. The robot therefore accommodates the Lithium battery with a better protection. Moreover, possible interference of the battery and the legs is therefore eliminated.

7.3 Wireless Communication

The robot pelvis accommodates a Netgear Nighthawk X10 R900 wireless communication router, that is placed on the back side of the torso, allowing for effective positioning of the router antenna to achieve reliable signal transmission and reception when the torso moves around the pelvis.

8 CENTAURO Control Architecture

The decentralized controller of the actuators is developed based on an impedance control scheme utilizing motor positions θ and velocity $\dot{\theta}$, and measured joint torque τ, displayed in Fig. 14. The inner most loop carry out the control of measured current i using a Proportional-Integral (PI) controller, with compensation of back-electromagnetic force (back-emf) effects and addition of a voltage feed-forward term. The controller reference value is set by the torque controller based on a Proportional-Derivative (PD) regulator and a torque state feedback, in addition to a friction compensation scheme [15, 14]. To respect the mechanical position limit of joints, we implement the “sand box” module: a one-directional stiffening PD position controller that is activated when the joint position is approaching the end limit, and prevents the joint position from meeting the mechanical stop.

While the lower-level joint controllers are executed on a dual-core microcontroller of individual actuators, the middle layer and higher-level control architecture of the CENTAURO robot relies upon four computation units: a COM Express module as motion PC, two Steam Box machines handling Vision/Perception data and higher-level controllers, and a Desktop computer as pilot PC. A high level schematic of the interconnections of the prototype control, actuation and perception components is shown in Fig. 15. The communication of the higher-level controllers with onboard PCs including Motion PC and Perception/Vision PCs is through a GigaBit Ethernet interface. The motion PC manages the data-broadcasting and

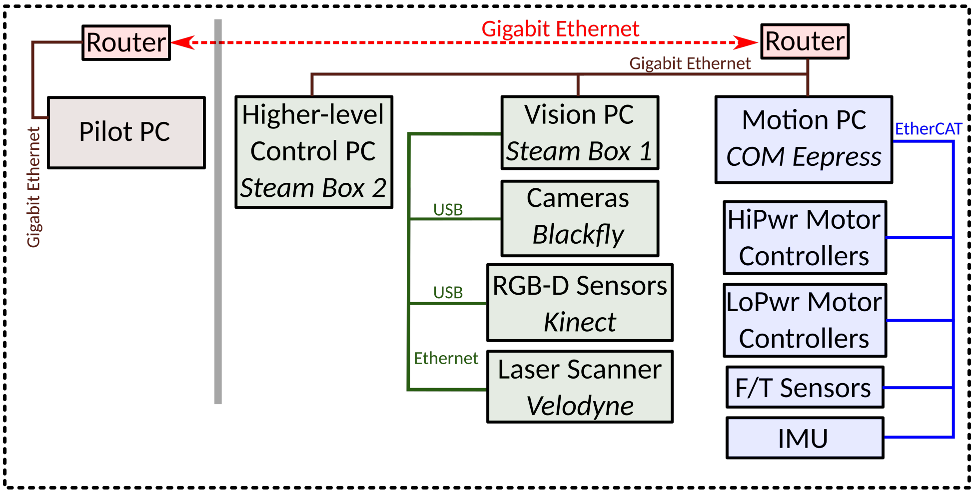

Figure 15: High level schematic of the interconnections of the CENTAURO prototype control, actuation and perception components.

centralized actuator control via real-time EtherCAT communication with both high and low power actuators' controllers, the Inertial Measurement Unit (IMU) and the Force/Torque (F/T) sensors. The vision PC is dedicated to the vision sensors acquisition, including three Point Grey Blackfly cameras, a Kinect-2 R-GBD sensor and a Velodyne LiDAR laser scanner, through USB and Ethernet connections.

For the control of the Centauro platform, we developed XBotCore (Cross-Bot-Core), a light-weight, real-time (RT) software platform for robotics [13]. XBotCore is open-source and is designed to be both an RT robot control framework and a software middleware. It satisfies hard RT requirements, while ensuring a 1 kHz control loop even in complex multi-DoF systems. The XBotCore Application Programming Interface (API) enables an easy transfer of developed software components to multiple robot platforms (cross-robot feature), inside any robotic framework or with any kinematics/dynamics library as a back-end. Out-of-the-box implementations are available for the YARP and ROS software frameworks and for the RBDL and iDynTree dynamics libraries. A Robot Hardware Abstraction Layer (R-HAL) that permits to seamlessly program and control any robotic platform powered by XBotCore is also provided by the framework. Moreover, a simple and easy-to-use middleware API, for both RT and non-RT control frameworks is available. The XBotCore API is completely flexible with respect to the external control framework the user wants to utilize.

As shown in 16, *XBotCore* spawns three threads in the Linux Xenomai[2] RTOS:

- The R-HAL RT thread is running at 1 kHz and is responsible to manage and synchronize the EtherCAT slaves in the robot, i.e. the electronic boards responsible for motor control and sensor data acquisition.
- The Plugin Handler RT thread is running at 1 kHz and is responsible to start all the loaded plugins, execute them sequentially and close them before unload. It is possible to dynamically load and unload one or more plugins in the Plugin Handler. As an example, the above mentioned RT Cartesian control plugin is running inside the Plugin Handler. A shared memory communication mechanism is used to share data between this component and the R-HAL at 1 kHz.
- The Communication Handler non-RT thread is running at 200 Hz and is responsible for the communication with external frameworks. This component provides the option

[2] https://xenomai.org

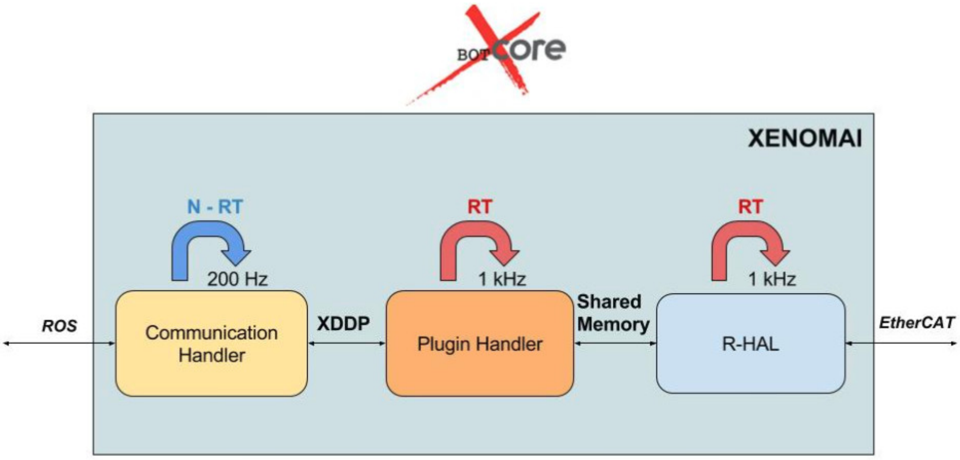

Figure 16: *XBotCore* threads and communication architecture.

to send the desired robot state from the non-RT API to the chosen communication framework and to receive the reference, respectively. The Communication Handler uses XDDP (Cross Domain Datagram Protocol) for the asynchronous communication between RT and non-RT threads, guaranteeing a lock-free IPC (Inter-Process Communication). The run loop of this component is quite simple: it updates the internal robot state using the XDDP pipe with the non-RT robot API, sends the robot state to all the communication frameworks, receives the new reference from the requested ”master” (we avoid to have multiple external frameworks commanding the robot) and finally, sends the received reference to the robot using the XDDP non-RT robot API.

9 Conclusions

This deliverable presented the final realization of the CENTAURO robot prototype. After the first iteration of the robot was designed and presented in D 2.3 [1], and evaluated in D 8.2 and D 8.3 [4, 2], some of the robot components were revised to improve the robot robustness and functionality based on feedback received during the first evaluation.

References

[1] Navvab. Kashiri, Houman. Dallali, and Nikos Tsagarakis. D2.3: First Prototype of CENTAURO Robot. 2017.

[2] Uwe Suss, Klas Nordberg. D8.3: First CENTAURO system evaluation. 2017.

[3] Zeyu Ren, Navvab Kashiri, Chengxu Zhou, Nikos G. Tsagarakis. HERI II: A Robust and Flexible Robotic Hand based on Modular Finger design and Under Actuation Principles. In *IEEE/RSJ International Conference on Intelligent Robots and Systems*, 2018.

[4] K. Nordberg, M. Felsberg, K. Holmquist, F. Jaremo-Lawin, A. Robinson, A. Frisoli, N. Kashiri, N. Tsagarakis, L. Muratore, M. Solazzi, D. Buongiorno, D. Chiaradia, M. Sarac, X. Chen, F. Schilling, M. Schwarz, T. Klamt, D. Pavlichenko, T. Cichon, C. Schlette, S. Behnke. D8.2: Core Component Evaluation. 2016.

[5] Lorenzo Baccelliere, Navvab Kashiri, Luca Muratore, Arturo Laurenzi, Malgorzata Kamedula, Alessio Margan, Stefano Cordasco, Jörn Malzahn, Nikos Tsagarakis. Development of a Human Size and Strength Compliant Bi-Manual Platform for Realistic Heavy Manipulation Tasks. In *IEEE/RSJ International Conference on Intelligent Robots and Systems*, 2017.

[6] Navvab Kashiri, Arash Ajoudani, Darwin G. Caldwell, and Nikos G. Tsagarakis. Evaluation of Hip Kinematics Influence on the Performance of a Quadrupedal Robot Leg. In *International Conference on Informatics in Control, Automation and Robotics*, volume 1, pages 205–212. scitepress, 2016.

[7] Lorenzo Baccelliere, Navvab Kashiri, Luca Muratore, Arturo Laurenzi, Małgorzata Kamedula, Alessio Margan, Stefano Cordasco, Jörn Malzahn and Nikos G. Tsagarakis. Development of a Human Size and Strength Compliant Bi-Manual Platform for Realistic Heavy Manipulation Tasks. In *IEEE/RSJ International Conference on Intelligent Robots and Systems (IROS)*. 2017.

[8] Navvab Kashiri, Jorn Malzahn, and Nikos Tsagarakis. On the Sensor Design of Torque Controlled Actuators: A Comparison Study of Strain Gauge and Encoder Based Principles. *IEEE Robotics and Automation Letters*, 2(2):1186–1194, 2017.

[9] Navvab. Kashiri, Houman. Dallali, and Nikos Tsagarakis. D2.1: Design concept of CENTAURO robot. 2015.

[10] Malgorzata Kamedula, Navvab Kashiri, Darwin G. Caldwell, and Nikos G. Tsagarakis. A Compliant Actuation Dynamics Gazebo-ROS Plugin for Effective Simulation of Soft Robotics Systems: Application to CENTAURO Robot. In *International Conference on Informatics in Control, Automation and Robotics*, volume 2, pages 485–491, Lisbon, Portugal, 2016.

[11] Navvab Kashiri, Nikos G Tsagarakis, Matteo Laffranchi, and Darwin G Caldwell. On the stiffness design of intrinsic compliant manipulators. In *IEEE/ASME International Conference on Advanced Intelligent Mechatronics*, pages 1306–1311, 2013.

[12] Navvab Kashiri, Arash Ajoudani, Darwin G. Caldwell, and Nikos G. Tsagarakis. Evaluation of Hip Kinematics Influence on the Performance of a Quadrupedal Robot Leg.

In *International Conference on Informatics in Control, Automation and Robotics*, volume 1, pages 205–212. scitepress, 2016.

[13] Luca Muratore, Arturo Laurenzi, Enrico Mingo Hoffman, Alessio Rocchi, Darwin G. Caldwell, and Nikos G. Tsagarakis. XBotCore: A Real-Time Cross-Robot Software Platform. In *IEEE International Conference on Robotic Computing*, 2017.

[14] Luc Le Tien, Alin Albu-Schaffer, Alessandro De Luca, and Gerd Hirzinger. Friction observer and compensation for control of robots with joint torque measurement. pages 3789–3795. IEEE, 2008.

[15] Kenji Kaneko, Shin'ichi Kondo, and Kouhei Ohnishi. A motion control of flexible joint based on velocity estimation. In *Annual Conference of IEEE Industrial Electronics Society*, pages 279–284, 1990.